

**Appraisal of geochemical composition and hydrodynamic sorting of the river
suspended material: Application of time-integrated suspended sediment sampler in a
medium-sized river (the Sava River catchment)**

Mavro Lučić^a, Nevenka Mikac^a, Niko Bačić^a, Neda Vdović^{a*}

^a Division for Marine and Environmental Research, Ruđer Bošković Institute, Bijenička cesta
54, 10000 Zagreb, Croatia

Mavro.Lucic@irb.hr, Nevenka.Mikac@irb.hr, Niko.Bacic@irb.hr

*corresponding author, Neda.Vdovic@irb.hr

ABSTRACT

1 The suspended particulate matter (SPM) carried by the rivers shows a wide range of particle
2 size classes, mineralogical and chemical compositions and is mainly influenced by
3 hydrodynamic sorting and provenance during the transport. Here, we have investigated the
4 composition of the SPM in the Sava River and its tributaries (Ljubljanica, Savinja and
5 Krapina) using a time-integrated mass flux sampler (TIMS). The representativeness of
6 material collected by TIMS was evaluated comparing fine-grained sediments, single-point
7 SPM and SPM collected using a shallow and deep-positioned sampler. The main results
8 have revealed that the mineralogical and geochemical composition of the material is largely
9 dependent on hydrological conditions. The differentiation of element composition is
10 especially emphasized at low water stage when most of the SPM consists of slow-settling
11 mineral phases (clay minerals and metal oxyhydroxides) which can be trapped in the
12 sampler. During periods of high discharges, differentiation is less prominent, and
13 homogenization of the SPM occurs, mainly as a part of bed load is also taken into

14 suspension. These conditions have proven unfavorable for sampler efficiency, as at least
15 part of the finest particles could not be retained. Additional issues that may occur during
16 TIMS employment relate to biologically driven carbonate precipitation, which is triggered by
17 changes in physico-chemical conditions at low water table in the summer period. Increased
18 concentration of Ca, related to that process, influences the elemental composition of the
19 SPM, which is particularly important when anthropogenic impact or sediment source is
20 assessed. Hence, in order to interpret the geochemical and mineralogical data collected by
21 TIMS, these factors should be taken into account. Our findings emphasize the need for
22 detailed studies of chemical composition of the SPM (time-integrated) in medium-sized rivers
23 and point out the significance of evaluating sampling representativeness during different
24 hydrological conditions.

25 Keywords: Geochemical composition; Hydrodynamic sorting; Time-integrated sampler; the
26 Sava River catchment

27 **1. Introduction**

28 The suspended particulate material (SPM) refers to particles that suspend in the water
29 column with a lower size limit of 0.20 or 0.45 μm in median diameter (Viers et al. 2009). It
30 consists of inorganic (quartz, feldspars, carbonates, clay minerals, metal oxyhydroxides,
31 heavy minerals) and organic (microorganisms and detritus) particulate matter (Gregory,
32 2006; Garzanti et al., 2011) usually presented in flocculated form (Droppo and Ongley,
33 1994). The SPM has a major role in transfer of elements from source to sink. According to
34 Horowitz (1991) and Audry et al. (2004), more than 90% of the riverine flux of metals is
35 associated with fine-grained sediment. So, when dealing with the trace elements
36 input/transfer/transport along a river, the investigation should focus on the SPM. However,
37 most of the SPM-bound element load is related to high flow events which are extremely
38 irregular. Another difficulty is to collect a representative sample and sufficient amount of the
39 SPM for analyzing different chemical and/or physical characteristics. In order to meet these
40 requirements, Phillips et al. (2000) developed a time-integrated suspended sediment sampler

41 (TIMS), mainly designed for streams and small lowland rivers (Schindler Wildhaber et al.
42 2012; Smith and Owens, 2014). Heretofore, TIMS was used in different studies (Russel et
43 al., 2000; McDonald et al., 2010; Droppo et al., 2019) and proven effective in several
44 environmental and controlled laboratory conditions (Martínez-Carreras et al. 2012; Marttila et
45 al. 2013; Perks et al., 2014). The amount of material collected was found sufficient and the
46 representativeness of TIMS was also proven satisfying. The main objections were the poor
47 assessment of the SPM mass flux (Goharrokhi et al., 2019) and lack of knowledge of how it
48 operates in larger river systems (Smith and Owens, 2014).

49 TIMS was also used in our previous research (Lučić et al., 2019) to investigate the Sava
50 River SPM and associated anthropogenic impact. The TIMS was set at one location in the
51 Sava River in Zagreb during different discharge periods. The results have shown increased
52 concentrations of some ecotoxic elements (As, Bi, Cd, Cr, Ni, Pb, Sb, Zn). Some issues
53 opened during that investigation: the input of the material from different sources during
54 different discharge periods and high concentration of calcite in spring sampling period was
55 observed. A possibility of *in situ* calcite precipitation instigated by algal bloom was
56 hypothesized.

57 This investigation has been conducted in order to obtain more information on the
58 hydrodynamic sorting and representativeness of the SPM (time-integrated) transported in a
59 medium size river. The case study was the Sava River and main tributaries (Ljubljana,
60 Savinja and Krapina) between its source and the city of Zagreb, as an example of medium
61 size river in the anthropogenically impacted environment. The aims of the study were:

- 62 1. to characterize the spatial and time variation of the geochemical composition of the
63 SPM sampled by TIMS in different hydrological conditions,
- 64 2. to assess potential influence of hydrodynamic sorting on suspended material,
- 65 3. to determine possible differences between shallow and deeper suspended load using
66 two TIMS samplers at one location.

67

68

69 2. Materials & methods

70 2.1. Study area

71 The Sava River is a major Danube tributary which flows through Slovenia and Croatia,
72 alongside the northern border of Bosnia and Herzegovina, and finally through Serbia. The
73 upper course of river is 232 km long with drainage basin covering 12680 km² of surface area
74 (Table 1). Other detailed geographical characteristics of the Sava River can be found in our
75 previous work (Lučić et al., 2019).

76

77 **Table 1** Main characteristics of studied rivers (average discharge refers to the outlet of the river)

Rivers	Basin area (km ²)	Length (km)	Average Discharge (m ³ s ⁻¹)	Average slope (m/km)	Annual sediment runoff Gg (m ²)
Sava (Radovljica)	909	55	44.9	-	192
Sava (Rugvica)	12680	232	310	200	-
Ljubljanica	1884	41	57.3	158.8	70
Savinja	1849	93.9	41.5	272	145
Krapina	1237	66.9	10.9	143.7	179

78

79 The Sava River has its origin as two branches, the Sava Dolinka and Sava Bohinjka rivers
80 which flow mainly through carbonate terrain (limestone and dolostone) until their confluence
81 at the city of Radovljica. From there, the river passes through previously deposited fluvio-
82 glacial terraces which alternate with Paleozoic rocks consisting of shales, quartz sandstones
83 and conglomerates. Besides Permo-Carbonian clastic sediments, the central part of the Sava
84 section in Slovenia is composed of Triassic carbonates, together with Paleogene and
85 Neogene clastic rocks in the area before the border with Croatia (Placer, 2008). In Croatia,
86 the drainage area of the river comprises terraced Quaternary deposits consisting of sands,
87 marls and clays (Šikić et al., 1979).

88 The Ljubljanica River flows through Ljubljana Moor, paleo-swamp filled with Quaternary
89 alluvial sediments (pebble, sand and clay) covering Paleozoic basement and Mesozoic
90 limestone and dolostone. Because of the considerable thickness of fluvio-glacial sediments,
91 the Ljubljansko Barje is one of the most important aquifers in Slovenia (Cerar and Urbanc,
92 2013).

93 The Savinja River, the second longest Slovenian river originates in the Kamnik-Savinja Alps
94 in Triassic carbonates and flows through Oligocene tuffs and andesites, while in the lower
95 part drains the Triassic carbonates and Miocene sandstones. As a result of its runoff
96 characteristics, its catchment area contributes up to 40 % of the lower Sava River (in
97 Slovenia) discharge in high rainfall events (Kobold and Sušelj, 2005).

98 The Krapina River has its origin in the Paleogene and Neogene of the Panonnian Basin. On
99 the left side of the flow, the Krapina River is filled by many streams that drain the Medvednica
100 mountain, consisting of rocks of different ages (from Silurian to Quaternary age) (Galović and
101 Peh, 2014).

102

103 *2.2. Sampling and preparation of samples*

104 TIMS samplers used in this study were slightly modified with respect to the original design.

105 According to Perks et al. (2014), TIMS does not operate isokinetically under the flow

106 velocities below 0.55 m s^{-1} which may spoil representativeness of sampled material.

107 Therefore, we used modified larger inlet and outlet (6 mm diameter), while tube diameter was

108 110 mm in width. The samplers were positioned at five locations (Fig. 1, Table 2), protected

109 by metal cages and fixed by steel uprights. At Zagreb location, sampling was conducted

110 during a hydrological year with five campaigns organized from October 2016 to July 2017.

111 During the spring and summer period, two samplers were positioned simultaneously: one at

112 the bottom and another tied under the pontoon and sunk 30 cm below the water surface. The

113 intention was to collect and compare shallow and deeper suspended load at the same

114 location. The shallower channel of the Sava River at Radovljica site and tributaries did not

115 allow sampling on the vertical profile. Sampling frequencies at these locations (Sava -

116 Radovljica, Ljubljana, Savinja, Krapina) were less frequent; at least two sampling

117 campaigns were performed at each site.

118 **Figure 1.**

119

120 Besides suspended material collected by TIMS, in the period of time-integrated sampling at
 121 the Sava River, single-point samples of suspended material were also taken, as well as the
 122 bottom river sediments. The frequency of sampling is shown in Table 2.
 123 The sediments were sieved through a 63 µm sieve using ambient water. Single-point SPM
 124 samples were taken in plastic 6 L bottles and subsequently filtered in laboratory (0.45 µm
 125 cellulose acetate, Sartorius) and dried at 60°C. TIMS samples were transferred into glass
 126 beakers and left to settle; the supernatant was then carefully decanted.
 127 The supernatant, remaining after single-point SPM and TIMS samples were separated,
 128 filtered using in-line syringe cellulose nitrate filters (0.45 µm, Sartorius), transferred into 10
 129 mL Teflon tubes and acidified with nitric acid (supra pure 65%, Fluka) for determination of
 130 soluble elements (European Communities Environmental Objectives 2009; Gottler 2012).
 131 For all the analyses except particle size determination, a portion of each sample was freeze-
 132 dried (FreeZone 2.5; Labconco) and ground to fine powder using a ball-mill (Pulverisette 7;
 133 Fritsch).

134 **Table 2** Sampling schedule for SPM and sediment samples in each sampling campaign.

River	Sample	Location	Coordinates	Sampling period	Number of single-point samples	Number of sediment samples
Sava	ZG	Zagreb (Croatia)	N 45°47'08.1" E 15°57'21.9"	October.2016	4	1
				November.2016	4	1
				February.2017	4	1
				April.2017	5	2
				July.2017	5	1
Sava	SRAD	Radovljica (Slovenia)	N 45°47'08.1" E 15°57'21.9"	October.2016	4	1
				November.2016	4	1
Ljubljanica	LJ	Ljubljana-Podgrad (Slovenia)	N 46°04'23.2" E 14°38'09.7"	February.2017	1	2
				April.2017	2	2
				July.2017	1	1
				November 2017	1	1
Savinja	SV	Veliko Širje (Slovenia)	N 46°05'28.7" E 15°11'31.4"	February.2017	1	1
				April.2017	2	2
				July.2017	1	2
				November 2017	1	2
Krapina	KR	Zaprešić (Croatia)	N 45°50'23.4" E 15°49'36.3"	April 2017	/	2
				July.2017	2	1
				November 2017	/	1

135 2.3. Methods

136 Particle size distribution (PSD) was determined using a laser-based particle size analyzer
 137 (LS 13320; Beckman Coulter Inc.). The PSD was calculated using Mie theory of light

138 scattering (optical parameters: refractive index = 1.53; absorption index = 0.1). The mineral
139 composition was identified by X-ray powder diffraction using a Philips X-Pert MPD
140 diffractometer (40 kV, 40 mA, range scanned 4–63° 2 θ). Bulk composition of 10 TIMS and 7
141 sediment samples was determined. For 6 chosen TIMS samples, the clay fraction (< 2 μ m)
142 was separated by centrifugation and analyzed on oriented slides after being air-dried,
143 saturated by ethylene glycol, and heated for 1 h at 400° and 550 °C. Proportions of minerals
144 were evaluated semi-quantitatively using distinctive peak areas (Moore and Reynolds, 1997;
145 Kahle et al., 2002), weighted by Schultz (1964) empirical factors, which represents rough
146 estimate of mineral percentages.

147 Prior to geochemical analysis, sediment and TIMS samples were digested by a two-step
148 procedure (I-5 ml HNO₃ (65%, pro analysi, Kemika) + 1 ml HCl (37 %, VLSI Grade,
149 Rotipuran) + 1 ml HF (47-51%, supra pur, Fluka); II-6 ml H₃BO₃ (40 g l⁻¹, Fluka)) in the
150 Microwave digestion system Multiwave 3000 (Anton Paar). Due to small amount of sample,
151 single-point SPM samples were dissolved by modified procedure (I-4 ml HNO₃ + 1 ml
152 HCl + 0.2 ml HF; II-1.25 ml 40 g l⁻¹H₃BO₃).

153 Multi-elemental analysis of dissolved and particulate fraction was conducted using a High-
154 Resolution Inductively Coupled Plasma Mass Spectrometer (HR ICPMS), Element 2 (Thermo
155 Finnigan). Analytical quality control was provided by simultaneous analysis of blanks and
156 certified reference materials (Soil-NCS DC 77302 and Stream Sediment-NCS DC 73309) for
157 which good recoveries (90-100 %) were obtained, depending on the element measured.
158 Details of the method are provided in Fiket et al. (2017). For water samples measurement
159 uncertainty was better than \pm 3%.

160 The hydrological data were provided by Meteorological and Hydrological Service of Croatia
161 (DHMZ) and Slovenia (ARSO). Discharge measurements were performed by conventional
162 current meter method. The SPM concentration was measured daily by filtration of surface
163 water samples taken in the middle of the river course, 10 – 20 cm below the water level.
164 Statistical treatments were performed using a R package “robCompositions” while heat-maps
165 were designed in package “gplots” in R platform (R Core Team, 2017).

166 **3. Results and discussion**

167 *3.1. Hydrological and particle size characteristics*

168 Five sampling campaigns conducted in Zagreb encompassed a wide spectrum of discharges
169 and SPM trends (Fig. 2). Except for the calm summer period, all seasons were characterized
170 by at least one increase in water discharge followed by corresponding variation of the SPM
171 content. Compared to the Sava, Ljubljanica and Savinja rivers have revealed similar trends of
172 discharge fluctuations (Fig. A.1 and A.2). Somewhat different hydrological conditions were
173 observed for the Krapina River in which high SPM concentration did not always follow the
174 rise of the water level (Fig. A.3), mainly as a result of different sediment sources (Morehead
175 et al., 2003).

176 In the Sava River SPM (both in TIMS and single-point samples), and in sediment samples,
177 predominant particle-size fraction was silt, regardless of the sampling period (Table 3). Due
178 to insufficient quantity, particle size analysis was made only for a few of the single-point SPM
179 samples. Fine-grained sediments were dominated by finer particle size ranging from 11.1 to
180 34.7 μm , compared to single-point (19.6 – 56.3 μm) and TIMS samples (40.6 – 56 μm). After
181 organic matter removal, a notable increase in clay content and consequently lower mean
182 grain size (Mz) was observed in all samples. These changes were more pronounced in TIMS
183 samples than in fine-grained sediments, which indicates that the flocculation process took
184 place in the river channel. Also, lower Mz in treated sediments compared to TIMS samples
185 suggests that the part of the finest material carried in suspension could pass through the
186 sampler in a case of a high flow rate.

187 **Figure 2.**

188

189 For the other rivers, the sediment particle size showed comparable variations, Mz of the
190 Ljubljanica River ranging from 15.8 to 23.1 μm , similar to Savinja (15.4 – 23.2 μm) and
191 Krapina rivers (15.1 – 18.4 μm). Regarding TIMS samples, the ones from the Krapina River
192 had lower Mz (19.5 – 44.2 μm), compared to those from Savinja (24.7 – 71.6 μm) and
193 Ljubljanica rivers (64.9 – 102.3 μm). In all treated samples there was a decrease in Mz. The

194 largest deviations between sediment and TIMS samples were observed for the Savinja and
 195 Ljubljana rivers. The presence of coarser particles in TIMS of the Savinja River was a result
 196 of its stronger erosive power emphasized during the high water level when the part of bed
 197 load could also be taken into suspension (Singh, 2009). The abundance of sand-sized
 198 particles in all samples of the Ljubljana River was largely the effect of erosion of soil
 199 aggregates along the watercourse (Woodward and Walling, 2007).

200 Grain-size data obtained for the shallow (TMZG4) and deep-positioned (TMBZG4) TIMS of
 201 the Sava River did not differ substantially (Table 3) which was not the case in the summer
 202 sampling campaign; deep-positioned TIMS (TMBZG5) contained higher share of clay
 203 fraction. However, when treated samples were compared, Mz in shallow positioned TIMSs
 204 decreased substantially while no such effect was observed for deep-positioned TIMSs. This
 205 could be related to the transport of aggregated soil particles in shallow relative to deeper load
 206 which contained more sand consisting of quartz, carbonates, tectosilicates and heavy
 207 minerals.

208
 209 **Table 3** Particle size distribution (%), mean size (Mz), and median size (d50) of the non-treated SPM
 210 samples collected by TIMS (TM), bottom positioned TIMS (TMB), single-point SPM (SPM) samples
 211 and fine-grained sediments (SED). The results for chemically dispersed samples are also shown. The
 212 abbreviations refer to sampling locations.

	Non-treated					Chemically dispersed				
	Clay	Silt	Sand	Mz	d50	Clay	Silt	Sand	Mz	d50
TMZG1	7.9	73.8	18.3	44.3	20.2	23.2	71.4	5.4	18.8	8.1
SEDZG1	17.6	81.4	1.0	11.1	7.5	27.5	68.8	3.7	15.3	5.9
SPMZG1-1	5.9	66.8	27.3	56.3	29.0	/	/	/	/	/
SPMZG1-2	12.8	82.3	4.9	19.6	13.0	/	/	/	/	/
TMZG2	6.0	72.1	21.9	56.0	26.5	22.3	72.9	4.8	17.7	9.1
SEDZG2	15.6	81.8	2.6	15.7	9.1	24.9	73.1	2.0	15.1	8.4
SPMZG2-1	15.7	58.9	25.4	42.1	15.3	/	/	/	/	/
SPMZG2-2	15.1	75.8	9.1	23.0	10.7	/	/	/	/	/
TMZG3	7.2	77.7	15.1	48.9	17.9	37.3	60.7	2.0	12.2	6.0
SEDZG3	15.9	80.5	3.6	16.3	8.2	27.9	70.2	1.9	12.9	6.6
SPMZG3	9.1	72.7	18.2	51.7	18.1	/	/	/	/	/
TMZG4	9.5	72.1	18.4	40.6	20.7	22.8	67.9	9.3	23.7	10.2
TMBZG4	9.6	65.5	25.0	50.9	22.9	21.1	61.1	17.8	40.3	12.9
SEDZG4	10.8	76.1	13.1	34.7	16.8	24.0	72.7	3.3	16.7	8.0
SPMZG4	8.8	75.3	15.9	36.1	18.2	/	/	/	/	/
TMZG5	8.7	66.5	24.8	52.2	23.8	46.3	45.2	8.5	21.3	3.1
TMBZG5	15.2	78.7	6.1	21.6	9.6	30.7	62.9	6.4	18.8	7.5
SEDZG5	13.8	84.1	2.1	15.0	9.4	30.3	64.9	4.8	16.9	6.3
TMRAD1	9.0	63.7	27.3	72.6	25.5	/	/	/	/	/
SRAD1	9.6	63.5	26.9	43.5	40.1	/	/	/	/	/
TMRAD2	9.6	71.2	19.2	54.1	26.5	/	/	/	/	/

SRAD2	9.5	74.6	15.9	37.0	32.9	/	/	/	/	/
TMLJ1	6.5	71.2	22.3	64.9	19.8	35.7	56.5	7.8	23.1	7.3
SEDLJ1-1	15.0	82.3	2.7	15.8	9.1	/	/	/	/	/
SEDLJ1-2	13.5	81.5	5.0	18.8	10.3	32.7	61.7	5.6	19.9	7.5
TMLJ2	6.9	65.9	27.2	65.1	27.4	35.2	51.6	13.2	36.8	8.5
SEDLJ2-1	8.5	88.0	3.5	21.7	15.7	30.5	66.3	3.2	16.4	8.2
SEDLJ2-2	12.4	84.4	3.2	18.2	11.3	29.8	66.1	4.1	15.8	8.1
TMLJ3	5.6	54.7	39.7	102.3	40.0	65.2	27.1	7.7	17.2	0.2
SEDLJ3	10.4	86.5	3.1	19.2	12.7	35.9	60.5	3.6	13.9	5.7
TMLJ4	4.9	57.6	37.5	90.9	38.5	30.9	46.4	22.7	83.8	11.6
SEDLJ4-1	10.2	85.6	4.2	21.5	12.3	30.4	63.8	5.8	19.8	9.4
SEDLJ4-2	10.4	83.8	5.8	23.1	12.7	31.9	64.3	3.8	15.1	7.8
TMSV1	10.2	81.3	8.5	25.8	11.5	22.9	66.7	10.4	27.4	9.4
SEDSV1	10.8	82.3	6.9	23.2	14.4	26.3	69.6	4.1	18.1	7.8
TMSV2	17.4	73.9	8.7	24.7	10.2	20.1	66.8	13.1	30.5	11.5
SEDSV2-1	12.5	85.0	2.5	17.0	10.4	27.1	68.8	4.1	16.9	7.7
SEDSV2-2	13.7	83.4	2.9	16.4	9.6	/	/	/	/	/
TMSV3	10.6	77.5	11.9	29.7	16.7	33.3	62.9	3.8	14.1	6.4
SEDSV3	11.3	85.0	3.7	18.7	11.2	30.7	67.6	1.7	11.8	6.1
TMSV4	6.5	64.0	29.5	71.6	30.0	26.9	62.4	10.7	24.4	9.5
SEDSV4-1	12.8	85.5	1.7	15.4	10.2	29.9	68.6	1.5	12.5	6.9
SEDSV4-2	11.7	86.8	1.5	16.4	11.7	38.9	60.2	0.9	11.1	5.1
TMKR1	11.6	83.0	5.4	19.5	11.2	21.4	71.1	7.5	23.6	10.1
SEDKR1-1	10.6	87.5	1.9	15.8	10.6	/	/	/	/	/
SEDKR1-2	10.1	86.7	3.2	17.4	11.1	23.5	73.7	2.8	14.8	7.8
SPMKR1	21.9	61.4	16.7	28.2	12.9	/	/	/	/	/
TMKR2	8.0	79.5	12.6	31.1	17.9	31.6	57.9	10.5	26.9	8.5
SEDKR2	10.7	85.8	3.5	18.4	11.9	19.3	75.7	5.0	20.2	9.8
TMKR3	7.4	74.4	18.2	44.2	20.2	20.8	72.1	7.1	20.7	10.9
SEDKR3	12.2	85.8	2.0	15.1	9.6	22.4	72.8	4.8	17.9	9.2
SPMKR3	10.6	76.4	13.0	31.5	14.5	/	/	/	/	/

213

214 3.2. Mineralogical characteristics

215 The mineralogical composition of material carried by rivers usually reflects watershed

216 lithology. However, determination of provenance is not straightforward and compositional

217 variability of suspended sediment should be determined (Garzanti et al., 2010). The minerals

218 present in all analyzed samples were quartz, calcite, dolomite, phyllosilicates and feldspars

219 (Table 4).

220 The most abundant minerals in sediment samples of the Sava River were quartz, calcite and

221 dolomite. The dominance of each of them alternated, depending on the sampling period. In

222 general, the highest amount of quartz was found in deeper positioned samplers and two

223 shallow samplers from the late autumn and spring sampling campaigns, when the highest

224 flow rate and SPM concentration was recorded. Regarding shallow positioned TIMS, higher

225 quartz content probably resulted from stronger erosive power during high discharge. In

226 higher energy conditions it is assumed that material is not sufficiently differentiated, mainly

227 because of minimal chemical weathering and the dominance of physical erosion in the
 228 source area.

229 The origin of carbonates in the Sava River SPM and sediments is mostly detrital. Variation of
 230 dolomite content in TIMS samples can be related to both source supply and hydrodynamic
 231 sorting. Even though proportions of minerals represent a rough estimate of mineral
 232 percentages, higher dolomite content observed in sediments cannot be neglected. This may
 233 be attributed to higher density of dolomite which affects its accumulation in finer sand and
 234 coarser silt classes; more than quartz, feldspars and calcite (Garzanti et al., 2009; Garzanti
 235 and Ando, 2019). The origin of calcite could be double-natured. As assumed for the other
 236 minerals, in most of the sampling periods calcite was undoubtedly detrital in origin.

237 Nevertheless, the high content of calcite found in sediment (55%) and shallow positioned
 238 TIMS (69%) might be related to biologically mediated precipitation process (Olivier et al.,
 239 2011; Lučić et al., 2019) instigated in the summer period, which will be discussed in more
 240 later. The higher content of phyllosilicates in TIMS compared to sediments was observed in
 241 periods of lower water levels which suggests that phyllosilicates have preferential transport in
 242 surface load and have a good possibility to be retained in the sampler. Their low content
 243 recorded in the SPM and sediment samples of the first and final sampling campaign was a
 244 consequence of dilution effect, mainly controlled by calcite and quartz abundance. Feldspar
 245 minerals did not show any variation visible from mineralogical analyses.

246 **Table 4** Mineral composition of analyzed samples. The amount of minerals content is obtained semi-
 247 quantitatively using distinctive peak areas (Moore and Reynolds, 1997; Kahle et al., 2002).

	Quartz	Feldspars	Phyllosilicates	Calcite	Dolomite
TMZG1	30	5	11	38	17
SEDZG1	31	3	6	38	22
TMZG2	39	7	11	20	23
SEDZG2	21	8	14	24	33
TMZG3	31	5	18	38	8
SEDZG3	41	2	12	29	16
TMZG4	43	7	15	18	18
TMBZG4	46	6	15	14	19
SEDZG4	32	4	15	30	19
TMZG5	15	4	7	69	4
TMBZG5	49	5	5	28	13

SEDZG5	16	6	14	55	9
TMLJ2	52	4	22	15	7
SEDLJ2	36	7	22	15	20
TMS2	53	3	17	11	16
SEDSV2	41	6	19	18	16
TMKR1	57	11	28	1	3
SEDKR1	48	10	30	8	4

248 Clay mineral composition obtained for TIMS samples of the Sava River was characterized by
 249 prevalence of illite/mica minerals, followed by chlorite, smectite, kaolinite and vermiculite,
 250 presented only in the summer sampling period (Table A.1). The comparison of clay minerals
 251 in shallow and deeper positioned TIMS, showed a higher amount of illite/mica and the
 252 absence of kaolinite in the latter, which implies that kaolinite does not prefer deeper transport
 253 (Gippel, 1995).

254 The slightly lower carbonate content was detected in all tributary samples, as the
 255 consequence of more siliciclastic lithologies. All minerals showed opposite behavior relative
 256 to quartz. Additionally, TIMS samples had an increased quartz content compared to
 257 sediments. These results were corroborated with grain size analysis which reflected
 258 coarsening of the TIMS samples during high water stages.

259

260 3.3. Soluble element concentrations

261 Concentrations of 16 chemical elements, Li, Rb, Sr, V, Cr, Mo, Mn, Fe, Co, Ni, Cu, Zn, Cd,
 262 Al, Pb and As, were determined in water samples (Appendix B1). In general, there was no
 263 difference in Li, Rb, Sr, Cr, Mo, Ni, Cu, Zn, Cd, Pb and As concentrations between TIMS and
 264 river water. Among these elements, only Mo indicated strong anthropogenic influence,
 265 particularly in the Savinja River. Molybdenum concentrations were higher than 5 ug L^{-1} ;
 266 values much higher than reported elsewhere (Smedley et al., 2017; Vidmar et al., 2017). As
 267 opposed to the above mentioned elements, concentrations of V, Mn, Fe, Co and Al
 268 significantly varied, with higher concentrations inside TIMS, except for the Krapina River. On
 269 average, particularly high concentrations were observed in the Savinja ($\sim 1500 \text{ ug L}^{-1}$) and
 270 Krapina ($\sim 550 \text{ ug L}^{-1}$) rivers, values were much greater than the world average (34 ug L^{-1})

271 (Gaillardet et al., 2003). These deviations can be related to changes in the redox conditions
272 at the sediment-water interface, mostly for redox-sensitive elements as V, Mn, Fe and Co
273 (Balistrieri et al., 1994, Tribovillard et al., 2006). The change of redox conditions inside the
274 sampler is probably the consequence of the degradation of organic matter which
275 continuously accumulates throughout the sampling period. The reaction of oxygen with
276 organic matter will occur until one of these two components is completely consumed resulting
277 in an increasing concentration of dissolved redox-sensitive elements or contribution of
278 colloidal fraction that can be found in <0.45 μm filtered water (Hill and Aplin, 2001; Morford,
279 2019).

280

281 *3.4. Geochemical composition of suspended material*

282 The geochemical composition (50 elements – major, trace and rare earth elements (REE)) of
283 the analyzed suspended sediments is given in the Appendix B2. The comparison of TIMS
284 samples showed a higher average Ca ($107342 \text{ mg kg}^{-1}$) and Mg (22761 mg kg^{-1})
285 concentrations in the Sava River than in TIMSs positioned at other locations (Ca – 68310 mg
286 kg^{-1} and Mg – 17716 mg kg^{-1}); the highest concentrations were observed during the summer
287 sampling period, which corroborated mineralogical records. Magnesium concentrations
288 proved to be sensitive to hydrodynamic sorting with the highest values in TIMSs during the
289 greatest discharge in the Sava (26482 mg kg^{-1}) and Savinja (27506 mg kg^{-1}) rivers. Other
290 major elements (Al, Fe, Ti, Na, K), being the part of aluminosilicates, showed the behavior
291 opposite of Ca and Mg, with the highest concentrations in samples of the Krapina River. The
292 REE and most of trace elements displayed the highest concentrations in samples with more
293 Al and Fe content.

294

295 *3.5. Correlation analysis*

296 Besides absolute element concentrations, geochemical data were also considered in terms
297 of their composite nature (Reimann et al., 2012). The principle of compositional data deems
298 each element as a part of a whole which holds only relative information and sums up to a

299 constant (Pawlowsky-Glahn et al., 2015). These closed data are mutually dependent, and
300 their relevant information rather lies in the ratios between parts of a whole. In order to follow
301 that definition, we used log-ratio transformation, called symmetric coordinates (balances),
302 where elements are arranged according to a clustering procedure (Kynčlová et al. 2017;
303 Reimann et al. 2017). The correlation analysis (Fig. 3) was conducted separately for all
304 analyzed types of samples; A) TIMS, B) single-point SPM and C) fine-grained sediments. In
305 these graphs, a similarity between TIMS and single-point SPM was observed. Fig. 3A (TIMS)
306 is characterized by two large clusters. Starting from the upper-right corner, elements indicate
307 their geogenic nature. Strong clustering is determined for Ga, Sc, V, Ni, Ge, Ti, Li, Al, Rb, K,
308 LREE, Th, HREE, Nb, Y, and to a lesser extent for Tl, U, Cs and Mg, which are mostly
309 detrital in origin. Here, Mg shows good correlation with both calcium and elements related to
310 aluminosilicate fraction which reflects its presence not solely in dolomite, but also its
311 incorporation into clay minerals (smectite) abundant in the studied rivers (Barth-Wirsching et
312 al., 1994). The second smaller subcluster consists of Fe, Na, and Cr, the presence of which
313 is assumed in multiple mineral phases (phyllosilicates, feldspars and heavy minerals). Sr and
314 Ca indicate their incorporation into the carbonate minerals, mostly calcite. The second large
315 cluster of elements (Co, Ba, Pb, As, Mn, Bi, Be, Cd, Mo, Sn, Sb, Zn, Cu and W) probably
316 emphasizes their anthropogenic nature and association with the finest particles (Chen et al.,
317 2014).

318 In a single-point SPM (Fig. 3B) elements such as LREE, Th, Ga, Li, HREE, Al, V, Y, Nb, Ti,
319 Sc, Cs, Tl, Ge, Rb, Co, Be, Ba, Na, W, Cr and Fe show moderate to strong mutual positive
320 correlation, which suggests their association with clay minerals, oxyhydroxides and organic
321 matter. Because most of the single-point samples were taken during low water level and
322 strictly in a shallow part of the flow, this group represents geogenic element association
323 dominating in a wash load where quartz, tectosilicates, heavy minerals and other fast-settling
324 phases are sparse. The last cluster consists of two smaller ones. The first one is carbonate
325 and feldspar related, and consists of U, Mg, Ca, Sr, K and Pb (Garçon et al., 2014); the
326 second one is dominated by mainly anthropogenic group of elements which tend to

327 concentrate in the finest part of shallow suspended load, such as Ni, Sn, Bi, Cd, Sb, As, Mn,
328 Cu, Zn and Mo.

329 The fine-grained sediments (Fig. 3C) display somewhat different clustering and not so
330 pronounced correlations. The upper-right corner suggests agglomeration of elements solely
331 detrital in origin. Moreover, the strong positive correlations of Ti, W, Nb, Ge and Na probably
332 suggest their presence in heavy minerals and tectosilicates which tend to concentrate in
333 deeper suspended load (Garzanti et al., 2011). The second smaller subcluster consists of
334 Ga, LREE, Li and Al mainly associated with clay minerals. An association of elements such
335 as V, Fe, Cr, Sc, As, Pb, Co, Sb, Y and HREE may imply mafic component, especially within
336 sediments of the Savinja and Krapina rivers (Salminen et al., 2005). The heat-map of fine-
337 grained sediments does not reveal a prominent anthropogenic association of elements.
338 Rather, they are positioned within the group of elements mostly related to phyllosilicates and
339 feldspars (Rb, Be, Tl, Cu, Bi, Th, K, Ba, Zn, Mn and Cs). The second large cluster consists of
340 two subclusters and point out carbonate components more dominant in the Sava River.
341 Association of elements Cd-Sn is partly influenced by anthropogenic impact. Except for Sn,
342 all grouped elements (Ni, Sr, U, Mg, Cd, Mo and Ca) have a similar ionic radius and can be
343 incorporated into carbonates (Rambeau et al., 2010; Lerouge et al., 2017)

344 **Figure 3.**

345

346 *3.6. Geochemical normalization*

347 To assess the representativeness of time-integrated sampler for sampling in the Sava River
348 and tributaries, we compared the geochemical composition of the SPM collected by shallow-
349 positioned TIMS to other sampled material (fine-grained sediment (< 63 μm), deep-
350 positioned TIMS and single-point SPM samples). In this way, important information about
351 geochemical similarity/dissimilarity between material captured in TIMS and other materials
352 present in a water column during different hydrological cycles could be attained. Single-point
353 SPM represents the current sample and we assumed the similarity to the material collected
354 by TIMS. During low discharges, the most of fine-grained sediment is settled to the bottom,

355 and clay/organic particles prevail in suspension. Somewhat different behavior can be
356 observed during the turbulent water conditions when most of the fine-grained sediment,
357 along with the part of fine sand, becomes the main component of the suspended load. Taking
358 into account these components, we have covered all the material on the vertical profile and
359 can reasonably conclude on the representativeness of the material collected by TIMS. The
360 cross-section sampling was not performed; it is assumed that fine-grained material is rather
361 homogeneously distributed across the horizontal profile (Walling et al. 2000; Perks et al.,
362 2014). The geochemical normalization of materials was performed using enrichment factor;
363 all elements in a single-point SPM (average concentrations of all samples except during high
364 water level) and fine-grained sediment were doubly-normalized to TIMS sample using a
365 formula:

$$366 \quad EF(E) = (E/Al)_{SPM/sediment} / (E/Al)_{TIMS} \quad [1]$$

367 where E is the element of interest normalized to insoluble element (Al) to minimize dilution
368 caused by quartz, carbonates or organic matter. Here, Al is chosen as a best reference non-
369 mobile element, which is not affected by hydrodynamic sorting (Garzanti et al., 2013). $EF > 1$
370 indicates enrichment of element compared to TIMS, while $EF < 1$ indicates a depletion.

371

372 *3.6.1. The Sava River*

373 The chemical composition of suspended sediment is usually subjected to changes
374 throughout the hydrological cycles (Viers et al., 2008). The temporal variability of flow can
375 cause sorting processes that are responsible for the geochemical differentiation of
376 suspended material based on hydrodynamic properties. During the first autumn sampling
377 campaign (Fig. 4A) the normalized elemental composition of sediment shows enrichment
378 pattern for Co, Sn and Pb. Even though all analyzed materials are under the anthropogenic
379 impact (Milačič et al., 2017), these anomalies suggest that the sediment is more influenced
380 by anthropogenic contamination than the SPM collected by TIMS. In addition, slight
381 enrichment of Cs, Be, LREE, Th, U, Mo, Fe, Ni, Cu, Zn, Ga and Tl in sediment compared to
382 TIMS is related to elements mainly hosted in micas or associated with clay, Fe-Mn

383 oxyhydroxides and organic matter, which indicates a minor loss of the suspended particles
384 from the sampler. Contrary to sediment, an average of elements in all single-point SPM
385 samples (average of 5 samples) shows lower concentrations of Na, Rb, Mg, Ca, Sr, Ba, Sc,
386 Y, Eu, Lu, Ti, V, Nb, Cr, W, Co, Ni, Ge, Sn, and higher concentrations of K, Be, Th, Mn, Zn
387 and Pb in relation to TIMS. The depletion of the first group of elements is caused by their
388 tendency to accumulate in deep suspended load (Garzanti et al., 2011; Bouchez et al., 2011;
389 Wu et al., 2013) and due to their hydrodynamic properties could be captured in the sampler
390 at high water level when the part of bed load is also taken in suspension. It is assumed that
391 Ca, Mg and Sr are mainly hosted in carbonates, Na, Sr and Eu in tectosilicates, while Lu, Ti,
392 Nb, Cr, Ni, Ge and Sn can be hosted partly in ultradense minerals. Higher enrichment of Mn
393 in single-point SPM is a result of its presence in clay minerals and oxyhydroxides, which
394 dominate in a shallow suspended load and are likely to escape from sampler. Nevertheless,
395 the normalized pattern of average SPM assumes reasonably good representativeness of
396 material collected by TIMS.

397 **Figure 4.**

398
399 The second autumn sampling campaign (Fig. 4B) is characterized by more extreme
400 hydrological conditions (Fig. 2). In that period, single-point SPM was sampled mostly at
401 medium discharges. When compared to TIMS, sediment displays a similar pattern as
402 observed in the previous period, i.e. minor enrichment of mostly geogenic (Na, Mg, REE and
403 Th) and some of anthropogenic elements (Ni, Zn, Cd, Sn, Pb and As). With respect to most
404 of the naturally-derived elements (from Li to Nb, W, Fe, Ga and Ge), average SPM values
405 show good similarity to TIMS. Moreover, the SPM at high water level does not show
406 significant enrichment which suggests that most of the material is captured inside the
407 sampler. Depletions of Mg, Ca, Sr could be explained by more siliciclastic supply in
408 conditions of high discharges, when the Sava River brings more material from the upper
409 reaches. Opposite variations of Mo, Mn, Cu, Zn and Cd during high and low water levels are
410 probably a consequence of their different source nature. During high discharges, the SPM is

411 mainly detrital in origin and metal-poor (Ollivier et al. 2011). Contrary, low water conditions
412 are characterized by metal-rich fraction which tends to adsorb onto clays, oxyhydroxides and
413 organic matter (Horowitz and Elrick, 1987; Baran et al., 2019). Based on that, we can
414 assume that TIMS sample represents averaged out SPM composition fairly well.

415 In the winter sampling period (Fig. 4C), single-point SPM samples were collected during low
416 discharges (Fig. 2). In these conditions, for most of the period, the lowest SPM concentration
417 was observed. Here, geochemical differences between different water stages are more
418 pronounced. High enrichment patterns for Mo, Mn, Ni, Cu, Zn, Cd, Sn, As, Sb and Bi at low
419 water stage may emphasize prominent instant anthropogenic input and preferable adsorption
420 onto clays/oxyhydroxides. During high discharges, siliciclastic and detrital influence is more
421 visible from the depletion of Mg, Ca and Sr in comparison to the previous sampling period.

422 Grain-size and mineralogical data suggest a good representativeness of material captured in
423 the sampler. This is because both analyses showed a higher amount of clay fraction and
424 phyllosilicates (Table 3 and 4) compared to sediment. Also, this is supported by no
425 enrichment patterns in average SPM for most of the geogenic elements (Li, Na, K, Rb, Cs,
426 Be, Ba, Sc, REE, Th, Ti, V, Nb, Fe, Ga and Ge). However, geochemical normalization of high
427 water SPM and sediment samples showed slight enrichments of REE and Th in relation to
428 TIMS. According to Garzanti et al., (2011) these elements can be enriched in both, shallow
429 and deeper suspended load, mainly as a result of provenance effect, concentration in
430 ultradense minerals, phyllosilicates and organic matter. Herein, we assumed that enrichment
431 in SPM/sediment sample could reflect instant provenance signal and scavenging of Th and
432 particularly MREE (Sm, Eu, Gd and Tb) onto Mn/Fe-oxyhydroxides and clays (Quinn et al.,
433 2006).

434 The spring sampling campaign (Fig. 4D) is characterized by calm hydrological conditions,
435 disturbed during the last three days of sampling (Fig. 2). In this period, the highest discharge
436 and SPM concentration were observed. The results obtained for sample from deep-
437 positioned TIMS corroborated previously stated inferences about hydraulic behavior of
438 elements; enrichment/accumulation of Na, Mg, Ca, Sr, Ba, Ti, Nb, Cr, Ge and Sn in the bed

439 load. Other enriched values of REE, V, Fe, Co, Ni and Cu suggest that these elements are
440 not solely dominant in a shallow load, but also partly transported in a deeper load hosted in
441 heavy minerals (Garzanti et al., 2011). Based on slight enrichment of mostly geogenic
442 elements (K, Rb, REE, U) in sediment and SPM at high water stage, together with lower
443 mean particle-size observed in sediment sample, a minor loss of finest particles from TIMS is
444 presumed. Similarly to previous sampling period, consecutive enrichments of Mo, Mn, Ni, Cu,
445 Zn, Cd, Sn and Pb are observed. This may suggest that comparing potentially anthropogenic
446 elements in different materials should be taken with care since this group of elements
447 represents fraction more sensitive to physico-chemical changes (pH, redox condition,
448 temperature, electric conductivity, a form of elements, etc.) in water. Therefore, in evaluating
449 time-integrated sampling in human-impacted rivers, focus should be put on naturally-derived
450 elements that are more stable and associated with the residual fraction (Aguilar-Hinojosa et
451 al., 2016; Baran et al., 2019).

452 As discussed earlier, the summer sampling period (Fig. 4E) was characterized by low
453 discharges and unusually high concentration of Ca in shallow positioned sampler.
454 Considering that Ca tends to accumulate in coarser sediment fraction, that may imply the
455 origin of Ca different than only detrital (Chen et al., 2014). An explanation could be intense
456 biological production at low water stage during which the elements are accumulated by the
457 long-chain organic acids (Rogerson et al., 2008). In addition, the slow-moving water
458 conditions in the sampler promoted biogenic calcite precipitation (Olivier et al., 2011), which
459 resulted in unusually high concentration of calcium. These processes invoked the
460 disturbance of the chemical composition of collected material which made the conclusion
461 about sampler's representativeness more difficult to reach. This is most apparent in higher
462 enrichments of all elements (except Ca and Mn) observed in the sediment which would mean
463 a notable loss of particles from the sampler that is in contradiction with other obtained results.
464 Namely, higher clay content and lower grain size determined in a shallow compared to
465 deeper Tims and sediment samples suggest good effectiveness of Tims that is most

466 probable to occur in these low water conditions. Therefore, an estimation of the chemical
467 composition in the summer sampling campaign should be interpreted with caution.
468 For the sampling location Radovljica (the Sava River headwaters), a smaller range of
469 elements was analyzed (Fig. 5.). The results of single-point SPM have emphasized enriched
470 patterns of mostly anthropogenic (Ni, Cu, Zn, Cd and Pb) and naturally derived (Rb, V and
471 Mn) elements. As aforementioned, these disparities are related to organic- and metal-rich
472 fraction abundant at low water levels. By observing grain-size distribution of the sediment
473 samples, TIMS could be evaluated as quite effective. Higher Cr values may reflect
474 anthropogenic impact (Milačić et al., 2017) or appearance of mafic minerals that concentrate
475 at the riverbed (Hinterlechner-Ravnik and Pleničar, 1967; Garzanti et al., 2011).

476 **Figure 5.**

477

478 3.6.2. Tributaries

479 The results of normalized diagrams of the Ljubljanica, Savinja and Krapina rivers have shown
480 somewhat different EFs compared to the Sava River (Fig. 6A, B and C). These tributaries
481 have a dissimilar morphology and shallower channels, which promotes coarser particles to
482 be collected by TIMS. Besides, the positioning of TIMS close to riverbed facilitates the
483 accumulation of coarse material regardless the variation of the hydrological cycle; the
484 increase of water level up to 2m is not uncommon. This can also explain high quartz content
485 determined in TIMS samples. Discrepancies found between single-point SPM and sediments
486 reflect the influence of hydrodynamic sorting on geochemical and mineralogical composition.
487 Because single-point SPM was collected only during low water stage, most of the particles
488 that contain geogenic elements are likely to be captured by TIMS.

489 TIMSs positioned in the Ljubljanica and Savinja rivers (Fig. 6A and B) were characterized
490 with higher concentration of Be and W, particularly in the summer period. The most probable
491 explanation would be their interaction with organic matter (Tuna et al., 2012; Boschi and
492 Willenbring, 2016) or the adsorption on the secondary Fe-Mn oxyhydroxides (Armiento et al.,

493 2013; Bauer et al., 2017), rather than the selective entrainment of heavy minerals (Garzanti
494 et al., 2010). As mentioned earlier, long-time sampling inside TIMS can probably cause a
495 change of physico-chemical conditions at the sediment-water interface. The reductive
496 dissolution of oxyhydroxide particles below this layer releases soluble Mn and induces its
497 upward moving into the water column but subsequently trapping it back as Mn oxides when
498 oxygenated water is encountered (Calvert and Pedersen, 1996; Tribovillard et al., 2006).
499 Inside the TIMS, this precipitation resulted in strong binding of Be and W with Mn, and
500 consequently their prominent depletions. This process could also be responsible for depletion
501 patterns of Mn, Pb, Zn, As and Sb observed in sediment samples in comparison to TIMS of
502 the Krapina River (Fig. 6C). As in the case of the Sava River, these variations can reflect
503 their sensitivity to physico-chemical changes at the boundary between sediment and the
504 overlying water (Baran et al., 2019). The higher EFs found in sediments for the most of
505 detrital elements (Cs, Ba, Sc, REE, Th, U, Ga) indicate that their main carriers are not easily
506 retained at high flow rate. This pertains particularly to the Savinja (Fig. 6B), as the
507 hydrologically most demanding river, in which higher loss of particles is expected. Since
508 Ljubljana and Krapina are typical lowland rivers with lower discharge and lower enrichment
509 patterns, more efficient retention of particles in TIMS is likely to occur.

510 **Figure 6.**

511

512 **4. Conclusions**

513 In this study, we have combined hydrological observations, granulometric, mineralogical and
514 geochemical data of the SPM in a medium-size river to characterize element behavior and
515 representativeness of material collected by time-integrated mass-flux sampler (TIMS). To
516 evaluate TIMS in real-environment conditions, we have compared different sampled
517 materials (SPM collected by TIMS, single-point SPM samples and fine-grained sediment (<
518 63 μm)). The main findings are as follows:

519 1. The flocculation process in the river channel induces coarser particle size in the single-
520 point SPM and the SPM collected by TIMS compared to fine-grained sediments (< 63 μm),

521 which otherwise represent their suitable representative. After organic matter removal, a
522 notable increase in clay content and lower mean grain size were observed.

523 2. The mineral composition of all samples is dominated by quartz, carbonates, phyllosilicates
524 and feldspars which are mainly detrital in origin. However, a high content of calcite in
525 sediment (55%) and shallow TMS (69%) determined in the summer period can be the result
526 of biologically instigated carbonate precipitation, supported by lower water table and almost
527 stagnant water conditions.

528 3. The geochemistry of analyzed materials is mostly influenced by the hydrodynamic sorting
529 and provenance; different compositions during different hydrological regimes are found. In
530 calm hydrological conditions, surface load shows enrichment patterns of partly anthropogenic
531 elements (Mo, Mn, Cu, Zn, Cd, As, Sb and Bi) adsorbed onto clay minerals, oxyhydroxides
532 and organic matter. The differentiation of suspended material is not observed at high water
533 stages when more detrital material is supplied and part of a bed load is re-suspended.

534 4. During low and medium water table, samplers at the Sava River proved to be a reasonably
535 good means of collecting representative time-integrated suspended material. However,
536 different chemical composition of shallow and deep-positioned sampler, induced by
537 hydrodynamic sorting, could be recognized. Somewhat problematic conditions can occur at
538 high flow rate due to partial loss of the clay fraction and variation of elemental composition,
539 particularly in human-impacted rivers. Therefore, using anthropogenic elements, mostly
540 bound to that fraction, to compare materials sampled in different periods, requires additional
541 caution. Moreover, changes in redox conditions and high biological activity in a summer
542 period can invoke additional modifications of the chemical composition of the material and
543 consequently distort the conclusion about the representativeness of the SPM. Hence, in
544 order to interpret geochemical and mineralogical data (time-integrated) in sediment source
545 modeling or assessing river sediment quality, these factors should be considered.

546

547

548

549 **Acknowledgements**

550 This work was supported by the Croatian Science Foundation under the project 7555
551 (TRACESS) and bilateral Croatian-Slovenian MSES project. The authors are grateful to Dr.
552 Ivo Lučić for his support in the field during the sampling campaigns as well as Mr. Roman
553 Trček's help on finding an appropriate location for TIMS positioning in the Savinja River.

554 **5. References**

- 555 Aguilar-Hinojosa, Y., Meza-Figueroa, D., Villalba-Atondo, A. I., Encinas-Romero, M. A.,
556 Valenzuela-García, J. L., Gómez-Álvarez, A., 2016. Mobility and bioavailability of metals in
557 stream sediments impacted by mining activities: the Jaralito and the Mexicana in Sonora,
558 Mexico. *Water Air Soil Poll* 227, 345.
- 559 Armiento, G., Bellatreccia, F., Cremisini, C., Ventura, G.D., Nardi, E., Pacifico, R., 2013.
560 Beryllium natural background concentration and mobility: a reappraisal examining the case of
561 high Be-bearing pyroclastic rocks. *Environ Monit Assess* 185, 559–572.
- 562 Audry, S., Schäfer, J., Blanc, G., Bossy, C., Lavaux, G., 2004. Anthropogenic components of
563 heavy metals (Cd, Zn, Cu, Pb) budgets in the Lot-Garonne fluvial system (France). *Appl*
564 *Geochem* 19(5), 769–786.
- 565 Balistrieri, L.S., Murray, J.W., Paul, B., 1994. The geochemical cycling of trace elements in a
566 biogenic meromictic lake. *Geochim Cosmochim Acta* 58, 3993–4008.
- 567 Baran, A., Mierzwa-Hersztek, M., Gondek, K., Tarnawski, M., Szara, M., Gorczyca, O.,
568 Koniarz, T., 2019. The influence of the quantity and quality of sediment organic matter on the
569 potential mobility and toxicity of trace elements in bottom sediment. *Environ Geochem Hlth*
570 41, 2893–2910.
- 571 Barth-Wirching, U., Klammer, D., Kovic-Kralj, P., 1994. The formation of analcime from
572 laumontite in the Smrekovec volcanics. *Environ. Earth Sci.* (2010) 59:951–956 955 123
573 Northwest Slovenia—an experimental approach. In: Weitkamp J, Karge HG, Pfeifer H,

574 Hoelderich W (eds) Zeolites and related microporous materials: state of the art 1994, Stud
575 Surf Sci Catal 84: 299–305.

576 Bauer, S., Blomqvist, S., Ingri, J., 2017. Distribution of dissolved and particulate
577 molybdenum, vanadium, and tungsten in the Baltic Sea. Mar Chem 196, 135–147.

578 Boschi, V., Willenbring, J.K., 2016. Beryllium desorption from minerals and organic ligands
579 over time. Chem Geol 439, 52–58.

580 Bouchez, J., Gaillardet, J., France-Lanord, C., Maurice, L., Dutra-Maia, P., 2011. Grain size
581 control of river suspended sediment geochemistry: clues from Amazon River depth profiles.
582 Geochem Geophys Geosy 12:Q03008.

583 Calvert, S.E., Pedersen, T.F., 1996. Sedimentary geochemistry of manganese: implications
584 for the environment of formation of manganiferous black shales. Econ Geol 91, 36–47.

585 Cerar, S. Urbanc, J., 2013. Carbonate Chemistry and Isotope Characteristics of Groundwater
586 of Ljubljansko Polje and Ljubljansko Barje Aquifers in Slovenia. Sci World J 2013, 1–11.

587 Chen, J.B., Gaillardet, J., Bouchez, J., Louvat, P., Wang, Y.N., 2014. Anthropophile elements
588 in river sediments: overview from the Seine River, France. Geochem Geophys Geosy
589 15:4526–4546.

590 Droppo, I.G., di Cenzo, P., Parrott, J., Power, J., 2019. The alberta oil sands eroded
591 bitumen/sediment transitional journey: influence on sediment transport dynamics, pah
592 signatures and toxicological effect. Sci Total Environ. 677, 718–731.

593 Droppo, I.G., Ongley, E.D., 1994. Flocculation of suspended sediment in rivers of south-
594 eastern Canada. Water. Res 28, 1799–1809.

595 European Communities Environmental Objectives (Surface Waters), 2009. Regulations S.I.
596 No. 272/2009.

597

598 Fiket, Ž., Mikac, N., Kniewald, G., 2017. Mass fractions of forty-six major and trace elements,
599 including rare earth elements, in sediment and soil reference materials used in environmental
600 studies. *Geostand Geoanal Res* 41, 123–135.

601 Gaillardet, J., Viers, J., Dupre, B., 2003. Trace elements in river waters. In: James I. Drever
602 (Ed.). Holland, H.D., Turekian, K.K. (Executive Editors), *Treatise on Geochemistry* vol 5:
603 *Surface and Ground Water, Weathering, and Soils*. Elsevier, 225–272.

604 Galović, L., Peh, Z., 2014. Eolian contribution to geochemical and mineralogical
605 characteristics of some soil types in Medvednica Mountain, Croatia. *Catena* 117, 145–156.

606 Garçon, M., Chauvel, C., France-Lanord, C., Limonta, M., Garzanti, E., 2014. Which minerals
607 control the Nd–Hf–Sr–Pb isotopic compositions of river sediments? *Chem Geol* 364, 42–55.

608 Garzanti, E., Andò, S., 2019. Heavy Minerals for Junior Woodchucks. *Minerals* 9, 148.
609 <https://doi.org/10.3390/min9030148>.

610 Garzanti, E., Ando, S., France-Lanord, C., Censi, P., Vignola, P., Galy, V., Lupker, M., 2011.
611 Mineralogical and chemical variability of fluvial sediments 2. Suspended-load silt (Ganga–
612 Brahmaputra, Bangladesh). *Earth Planet Sci Lett* 302, 107–120.

613 Garzanti, E., Andò, S., France-Lanord, C., Vezzoli, G., Galy, V., Najman, Y., 2010.
614 Mineralogical and chemical variability of fluvial sediments. 1. Bedload sand (Ganga–
615 Brahmaputra, Bangladesh). *Earth Planet Sci Lett* 299, 368–381.

616 Garzanti, E., Andò, S., Vezzoli, G., 2009. Grain-size dependence of sediment composition
617 and environmental bias in provenance studies. *Earth Planet Sci Lett* 277(3-4), 422–432.

618 Garzanti, E., Padoan, M., Andò, S., Resentini, A., Vezzoli, G., Lustrino, M., 2013. Weathering
619 and relative durability of detrital minerals in equatorial climate: sand petrology and
620 geochemistry in the East African Rift. *J Geol* 121, 547–580.

621 Gippel, C.J., 1995. Potential of turbidity monitoring for measuring the transport of suspended
622 solids in streams. *Hydrol Process* 9(1), 83–97.

623 Goharrokhi, M., Pahlavan, M., Lobb, D.A., Owens, P.N., Clark, S.P., 2019. Assessing issues
624 associated with a time-integrated fluvial fine sediment sampler. *Hydrol Process* 33, 15, 2048–
625 2056.

626 Gottler, R.A., 2012. Part 3000 metals. In: Rice, E.W., Braid, R.B., Eaton, A.D., Clesce, L.S.
627 (Eds.), *Standard Methods for the Examination of Water and Waste Water*, 22nd ed. Port City
628 Press, Baltimore, MD, USA pp. 3-1–3–11.

629 Gregory, J., 2006. *Particles in Water: Properties and Processes*. IWA Publishing/CRC.
630 Press, London, U.K.

631 Hill, D.M., Aplin, A.C., 2001. Role of colloids and fine particles in the transport of metals in
632 rivers draining carbonate and silicate terrains. *Limnol Oceanogr* 46(2), 331–344.

633 Hinterlechner-Ravnik, A., Pleničar, M., 1967. Smrekovski andezit in njegov tuf (The
634 Smrekovec andesite and its tuff – in Slovenian). *Geologija* 10, 219–237.

635 Horowitz, A.J., 1991. *A Primer in Sediment-trace Element Chemistry*. Lewis Publishers,
636 Chelsea, MA, USA.

637 Horowitz, A.J., Elrick, K.A., 1987. The relation of stream sediment surface area, grain size
638 and composition to trace element chemistry. *Appl Geochem* 2, (4), 437–451.

639 Kahle, M., Kleber, M., Jahn, R., 2002. Review of XRD-based quantitative analyses of clay
640 minerals in soils: the suitability of mineral intensity factors. *Geoderma* 109, 191–205.

641 Kobold, M., Sušelj, K., 2005. Precipitation forecasts and their uncertainty as input into
642 hydrological models. *Hydrol Earth Syst Sci* 9, 322–332.

643 Kynčlová, P., Hron, K., Filzmoser, P., 2017. Correlation between compositional parts based
644 on symmetric balances. *Math Geosci* 49, 777–796.

645 Lerouge, C., David, K., Claret, F., Debure, M., Grangeon, S., Madé, B., Montavon, G.,
646 Tournassata, C., 2017. Role of carbonate minerals in the distribution of trace elements in
647 marine clay formations. *Procedia Earth Planet Sci* 17, 798–801.

648 Lučić, M., Jurina, I., Ščančar, J. Mikac, N., Vdović, N., 2019. Sedimentological and
649 geochemical characterization of river suspended particulate matter (SPM) sampled by time-
650 integrated mass flux sampler (TIMS) in the Sava River (Croatia). *J Soils Sediments* 19, 989–
651 1004.

652 Martínez-Carreras, N., Krein, A., Gallart, F., Iffly, J.F., Hissler, C., Pfister, L., Hoffmann, L.,
653 Owens, P.N., 2012. The Influence of Sediment Sources and Hydrologic Events on the
654 Nutrient and Metal Content of Fine-Grained Sediments (Attert River Basin, Luxembourg).
655 *Water Air Soil Poll* 223, 5685–5705.

656 Marttila, H., Saarinen, T., Celebi, A., Kløve, B., 2013. Transport of particle-associated
657 elements in two agriculture-dominated boreal river systems. *Sci Total Environ* 461-462:693–
658 705.

659 McDonald, D.M., Lamoureux, S.F., Warburton, J., 2010. Assessment of a time-integrated
660 fluvial suspended sediment sampler in a high arctic setting. *Geogr Ann A*, 92A:225–235.

661 Milačič, R., Zuliani, T., Vidmar, J., Oprčkal, P., Ščančar, J., 2017. Potentially toxic elements
662 in water and sediments of the Sava River under extreme flow events. *Sci Total Environ* 605–
663 606, 894–905.

664 Moore, D., Reynolds, R., 1997. X-Ray-Diffraction and the identification and analysis of clay
665 minerals. Oxford University Press, New York.

666 Morehead, M.D., Syvitski, J.P., Hutton, E.W.H., Peckham, S.D., 2003. Modeling the temporal
667 variability in the flux of sediment from ungauged river basins. *Global Planet Change* 39(1-2),
668 95–110.

669 Morford, J.L., 2019. Redox-Sensitive Metals. in: *Encyclopedia of Ocean Sciences* 3rd
670 Edition, edited by: Cochran, J.K., Bokuniewicz, H.J., Yager, P.L. Elsevier/Academic Press,
671 323–327.

672 Ollivier, P., Radakovitch, O., Hamelin, B., 2011. Major and trace partition and fluxes in the
673 Rhône River. *Chem Geol* 285, 15–31.

674 Pawlowsky-Glahn, V., Egozcue, J. J., Tolosana-Delgado, R., 2015. *Modeling and Analysis of*
675 *Compositional Data*. London: John Wiley & Sons.

676 Perks, M.T., Warburton, J., Bracken, L., 2014. Critical assessment and validation of a time-
677 integrating fluvial suspended sediment sampler. *Hydrol Process* 28(17), 4795–4807.

678 Phillips, J.M., Russel, M.A., Walling, D.E., 2000. Time-integrated sampling of fluvial
679 suspended sediment: a simple methodology for small catchments. *Hydrol Process* 14, 2589–
680 2602.

681 Placer, L., 2008. Principles of the tectonic subdivision of Slovenia. *Geologija*, 51/2, 205–217.

682 Quinn, K.A., Byrne, R.H., Schijf, J., 2006. Sorption of yttrium and rare earth elements by
683 amorphous ferric hydroxide: influence of pH and ionic strength. *Mar Chem* 99, 128–150.

684 R core team, 2017. R: a language and environment for statistical computing. R Foundation
685 for statistical computing, Vienna, Austria URL <http://www.R-project.org>.

686 Rambeau, C.M.C., Baize, D., Saby, N.P.A., Matera, V., Adatte, T., Foellmi, K.B., 2010. High
687 Cadmium concentrations in Jurassic limestone as the cause for elevated cadmium levels in
688 deriving soils: a case study in Lower Burgundy, France. *Environ Earth Sci* 61, 1573–585.

689 Reimann, C., Filzmoser, P., Fabian, K., Hron, K., Birke, M., Demetriades, A., 2012. The
690 concept of compositional data analysis in practice – total major element concentrations in
691 agricultural and grazing land soils of Europe. *Sci Total Environ* 426, 196–210.

692 Reimann, C., Filzmoser, P., Hron, K., Kynčlová, P., Garrett, R.G., 2017. A new method for
693 correlation analysis of compositional (environmental) data – a worked example *Sci Total*
694 *Environ* 607–608, 965–971.

695 Rogerson, M., Pedley, H. M., Wadhawan, J. D., Middleton, R., 2008. New Insights into
696 Biological Influence on the Geochemistry of Freshwater Carbonate Deposits. *Geochim*
697 *Cosmochim Ac* 72, 4976–4987.

698 Russell, M.A., Walling, D.E., Hodgkinson, R.A., 2000. Appraisal of a simple sampling device
699 for collecting time-integrated fluvial suspended sediment samples. *International Association*
700 *of Hydrological Sciences* 263.

701 Salminen, R., Batista, M.J., Bidovec, M., Demetriades, A., De Vivo, B., De Vos, W., Duris, M.,
702 Gilucis, A., Gregorauskiene, V., Halamić, J., et al., 2005. FOREGS Geochemical Atlas of
703 Europe, Part 1: Background Information, Methodology and Maps. Geological Survey of
704 Finland.

705 Schindler Wildhaber, Y., Michel, C., Burkhardt-Holm, P., Bänninger, D., Alewell, C., 2012.
706 Measurement of spatial and temporal fine sediment dynamics in a small river. *Hydrol Earth*
707 *Syst Sc* 16, 1501–1515.

708 Schultz, L.G., 1964. Quantitative interpretation of mineralogical composition from X-Ray and
709 chemical data for the Pierre Shale. U. S. Geological Survey, Professional Paper 391-C.

710 Singh, P., 2009. Major, trace and REE geochemistry of the Ganga River sediments:
711 Influence of provenance and sedimentary processes. *Chem Geol* 266(3-4), 242–255.

712 Smedley, P.L., Kinniburgh, D.G., 2017. Molybdenum in natural waters: A review of
713 occurrence, distributions and controls. *Appl Geochem* 84, 387–432.

714 Smith, B.T., Owens, P.N., 2014. Flume- and field-based evaluation of a time-integrated
715 suspended sediment sampler for the analysis of sediment properties. *Earth Surf Proc Land*
716 39, 1197–1207.

717 Šikić, K., Basch, O, Šimunić, A., 1979. Geological Map of SFRJ in scale 1:100000.
718 Explanatory booklet to sheet Zagreb.- Federal Geological Survey, Beograd.

719 Tribovillard, N., Algeo, T., Lyons, T.W., Riboulleau, A., 2006. Trace metals as paleoredox
720 and paleoproductivity proxies: an update. *Chem Geol* 232, 12–32.

721 Tuna, G.S., Braida, W., Ogundipe, A., Strickland, D., 2012. Assessing tungsten transport in
722 the vadose zone: From dissolution studies to soil columns. *Chemosphere* 86, 1001–1007.

723 Vidmar, J., Zuliani, T., Novak, P., Drinčić, A., Ščančar, J., Milačič, R., 2016. Elements in
724 water, suspended particulate matter and sediments of the Sava River. *J Soils Sediments*
725 17:1917–1927.

726 Viers, J., Dupré, B., Gaillardet, J., 2009. Chemical composition of suspended sediments in
727 World Rivers: New insights from a new database. *Sci Total Environ* 407, 853–868.

728 Viers, J., Roddaz, M., Filizola, N., Guyot, J.L., Sondag, F., Brunet, P., Zouiten, C.,
729 Boucayrand, C., Martin, F., Boaventura, G.R., 2008. Seasonal and provenance controls on
730 Nd-Sr isotopic compositions of Amazon rivers suspended sediments and implications for Nd
731 and Sr fluxes exported to the Atlantic Ocean, *Earth Planet Sci Lett* 274, 511–523.

732 Walling, D.E., Owens, P.N., Waterfall, B.D., Leeks, G.J., Wass, P. D., 2000. The particle size
733 characteristics of fluvial suspended sediment in the Humber and Tweed catchments, UK. *Sci*
734 *Total Environ*, 251-252, 205–222.

735 Woodward, J., Walling, D.E., 2007. Composite suspended sediment particles in river
736 systems: their incidence, dynamics and physical characteristics. *Hydrol Process* 21, 3601–
737 3614.

738 Wu, W., Zheng, H., Xu, S., Yang, J., Liu, W., 2013. Trace element geochemistry of riverbed
739 and suspended sediments in the upper Yangtze River. *J Geochem Explor* 124, 67–78.

740

741 Figure caption

742

743 **Figure 1.** Map of sampling sites (map sourced from <https://maps-for-free.com/>).

744

745 **Figure 2.** Water discharge, suspended particulate matter (SPM) concentrations and timing of
746 collecting single-point SPM samples at the Zagreb sampling site during five sampling
747 campaigns (October and November 2016; February, April and July 2017). Data provided
748 from Meteorological and Hydrological Service.

749

750 **Figure 3.** Heat-maps of correlation coefficients based on symmetric coordinates for different
751 types of samples; A) TIMS, B) single-point SPM and C) fine-grained sediments. Samples
752 from all locations are included.

753

754 **Figure 4.** Doubly-normalized chemical composition of the fine-grained sediment and single-
755 point SPM from the Sava River, Zagreb. SPM average refers to at least four single-point
756 SPM samples. The samples are normalized to TIMS: A) first sampling campaign (October
757 2016); B) second sampling campaign (November 2016); C) third sampling campaign
758 (February 2017); D) fourth sampling campaign (April 2017); E) fifth sampling campaign (July
759 2017). The elements are arranged following the periodic table groups.

760

761 **Figure 5.** Doubly-normalized chemical composition of fine-grained sediment and single-point
762 SPM from the Sava River, Radovljica. The samples are normalized to TIMS: SRAD1 – first
763 sampling campaign (October), SRAD2 – second sampling campaign (November). The
764 elements are arranged following the periodic table groups.

765

766 **Figure 6.** Doubly-normalized chemical composition of fine-grained sediment and single-point
767 SPM at the tributaries. The samples are normalized to TIMS: A) the Ljubljanica River
768 (Podgrad); B) the Savinja River (Veliko Širje; C) the Krapina River (Zaprešić). The elements
769 are arranged following the periodic table groups.

770

771

772

773

Declaration of interests

The authors declare that they have no known competing financial interests or personal relationships that could have appeared to influence the work reported in this paper.

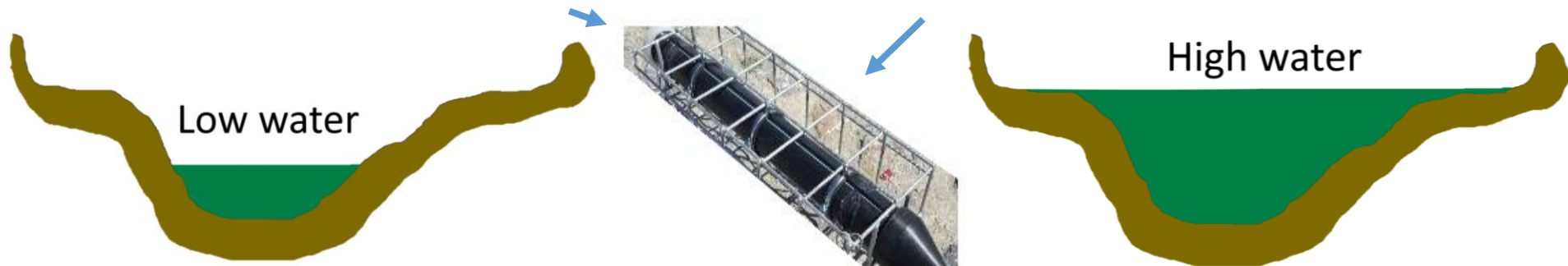
The authors declare the following financial interests/personal relationships which may be considered as potential competing interests:

Sava River



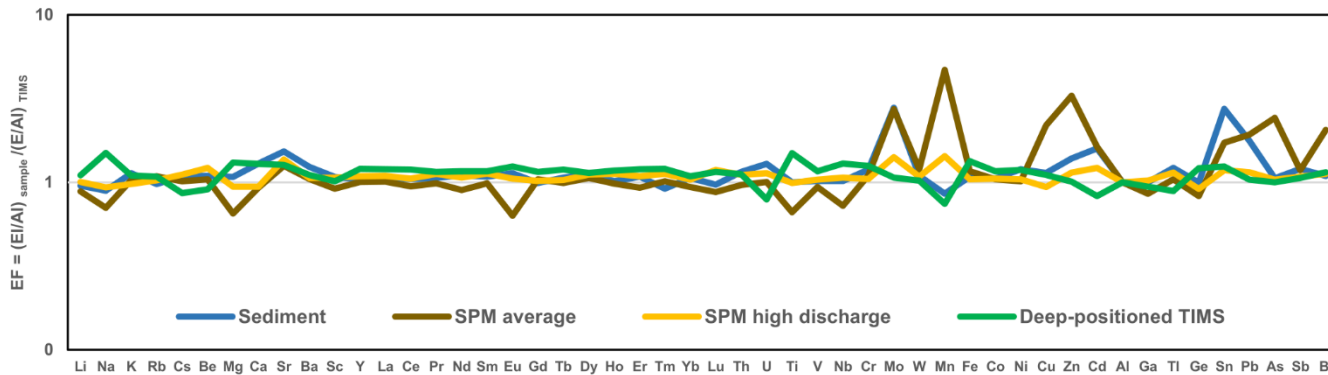
Good representativeness of SPM collected by TIMS

Lower capability to retain clay-rich particles in TIMS



SPM is abundant in clay minerals, oxyhydroxides and organic matter

Part of bed load is also re-suspended
Homogenization takes place



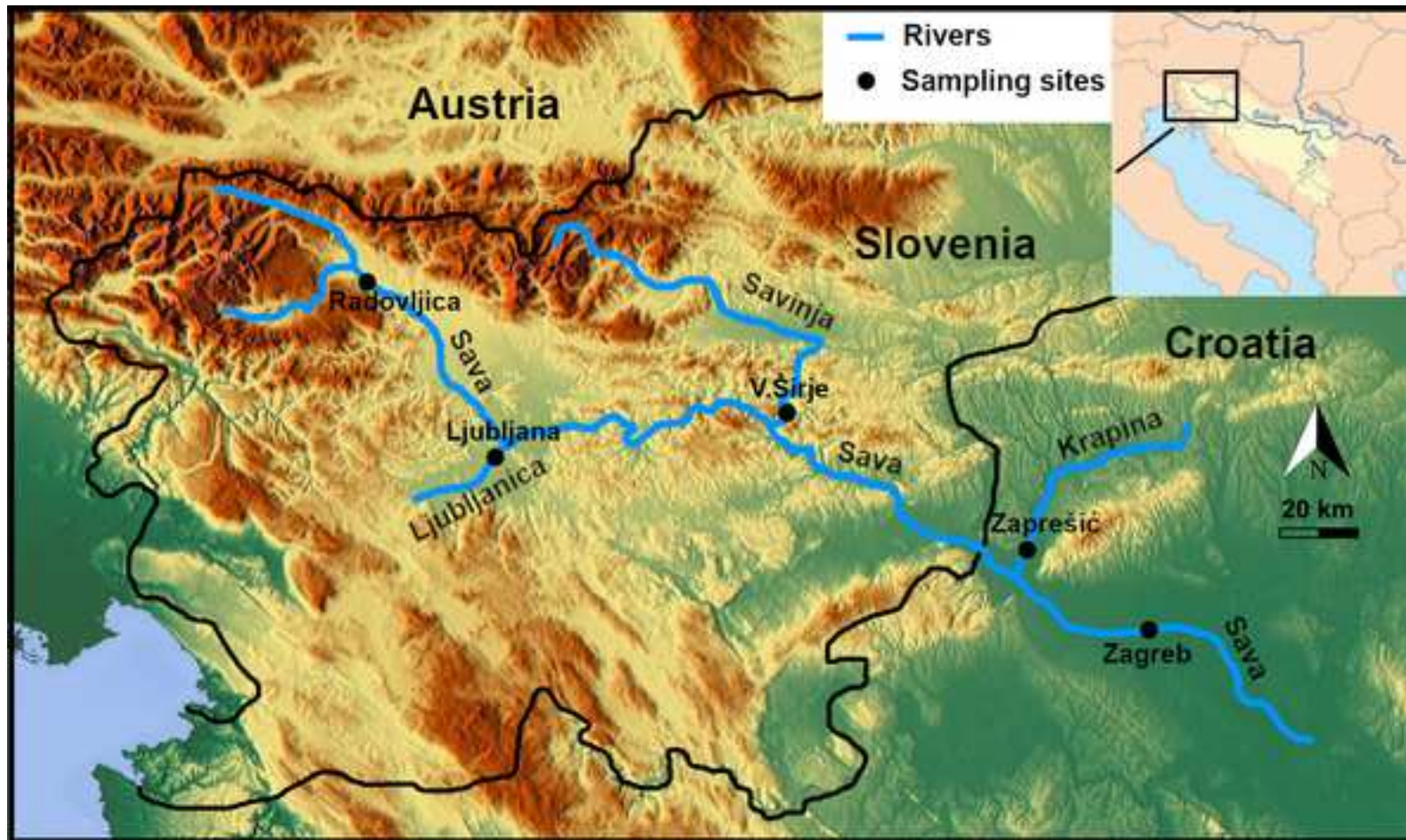
Supplementary material for on-line publication only

[Click here to download Supplementary material for on-line publication only: Lucic et al Appendix A.docx](#)

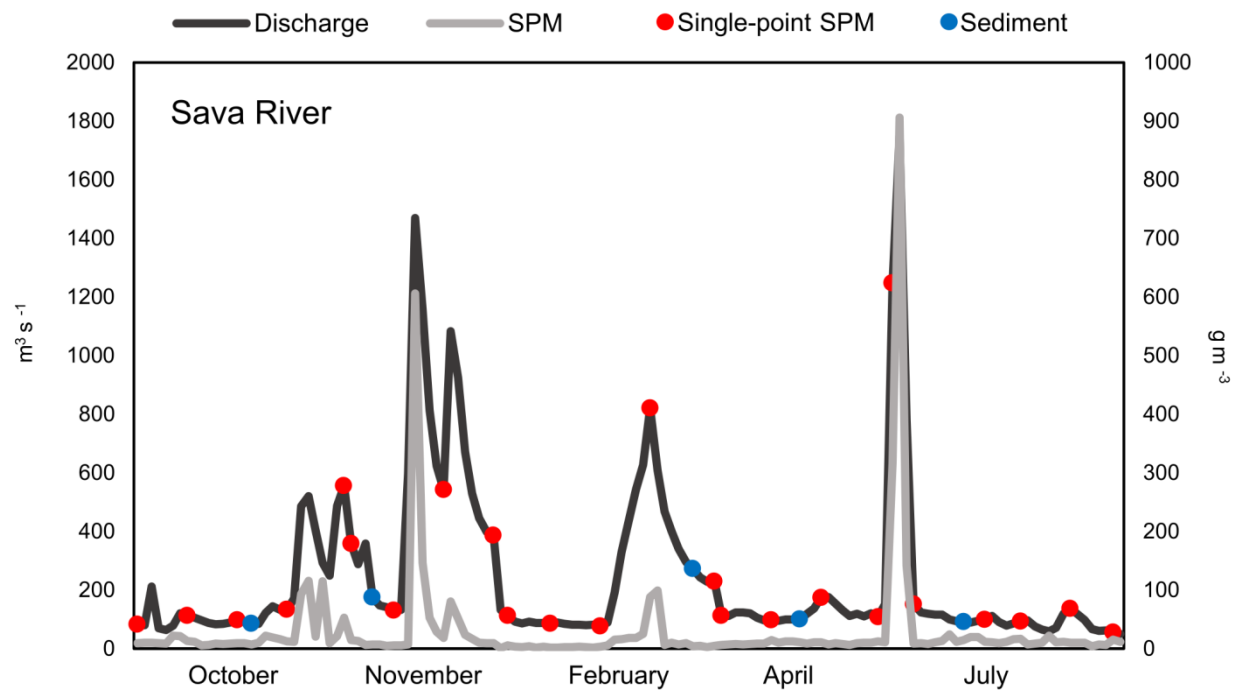
Supplementary material for on-line publication only

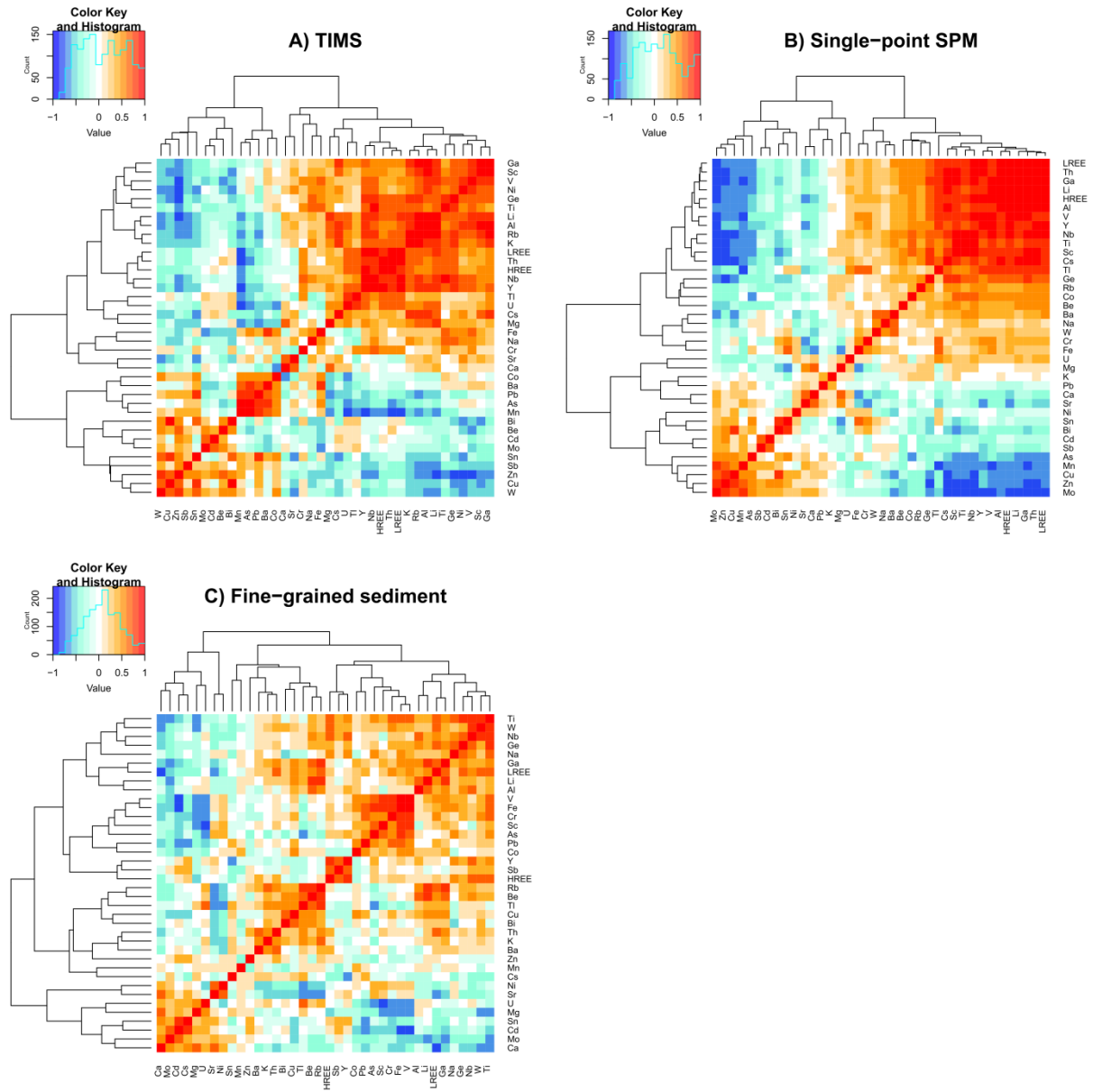
[Click here to download Supplementary material for on-line publication only: Lucic et al Appendix B.xlsx](#)

Figure
[Click here to download high resolution image](#)

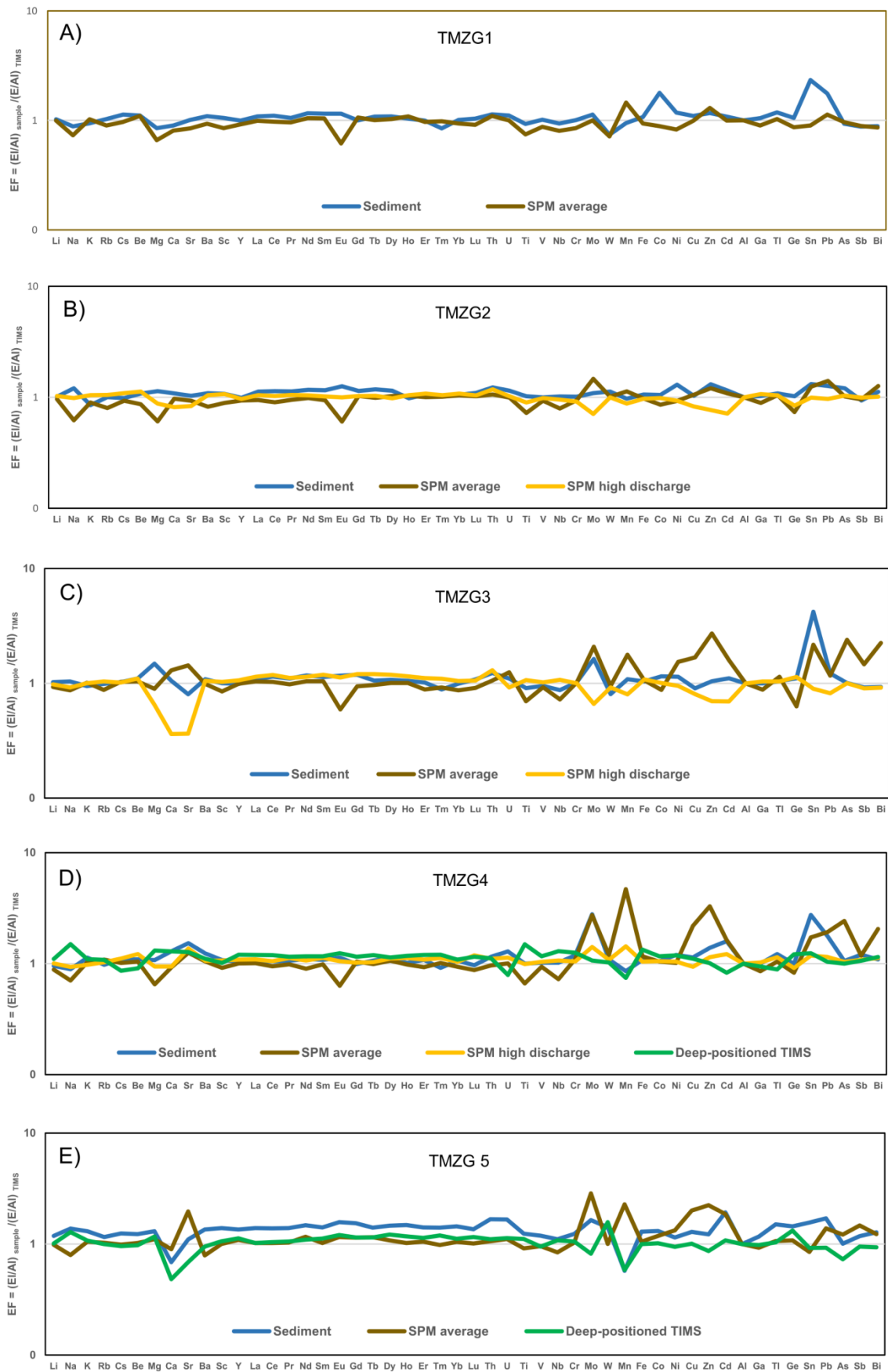


Figure





Figure



Figure

